The Prediction of Stress and Safety Factor of Shock Absorber Based on Cyclic Loading Using Finite Element Method

Endra Dwi Purnomo
Research Center for Process and Manufacturing Industry Technology, National Research and Innovation Agency of the Republic of Indonesia (BRIN)

Azka, Muizuddin
Research Center for Process and Manufacturing Industry Technology, National Research and Innovation Agency of the Republic of Indonesia (BRIN)

Hotma, Lambert
Research Center for Process and Manufacturing Industry Technology, National Research and Innovation Agency of the Republic of Indonesia (BRIN)

Aziz, Amiruddin
Research Center for Process and Manufacturing Industry Technology, National Research and Innovation Agency of the Republic of Indonesia (BRIN)

他

https://doi.org/10.5109/7162006

出版情報：Evergreen. 10 (4), pp.2456-2463, 2023-12. 九州大学グリーンテクノロジー研究教育センター
バージョン：

The Prediction of Stress and Safety Factor of Shock Absorber Based on Cyclic Loading Using Finite Element Method

Endra Dwi Purnomo[1], Muizuddin Azka[1,*], Lambert Hotma[1], Amiruddin Aziz[1], Khamda Herbandono[1], Nasril[1], Arifin[1]

[1]Research Center for Process and Manufacturing Industry Technology,
National Research and Innovation Agency of the Republic of Indonesia (BRIN),
South Tangerang, Indonesia 15314

*E-mail: muizuddin.azka@brin.go.id

(Received February 10, 2023; Revised September 27, 2023; accepted October 25, 2023).

Abstract: The aim of this study was to predict the strength of shock absorber under cyclic loading, with the goal of supporting the development of suspension components for electric vehicles. Shock absorber was designed with specific material specifications to effectively dampen vibrations and dissipate kinetic energy. The process began with the initial drafting of the geometric structure, followed by the determination of boundary conditions using cyclic loading forces. Furthermore, mesh grid independence and convergence tests were carried out to assess the accuracy of the simulation, using Finite Element Method (FEM) with ANSYS software. The simulation was conducted to analyze deformation, von Mises stress, and safety factor. The results showed that the mesh grid independence test and convergence test assisted in determining the appropriate mesh size for model optimization and efficiency. Additionally, FEM simulation provided stress and deformation values that could identify critical areas within the components. Another important result was the gradual decline in safety factor value, starting from the sixth second and continuing until the end of the simulation under cyclic loading conditions. This transient behavior of safety factor value should be taken into consideration for design safety.

Keywords: Shock Absorber, Cyclic Loading, Finite Element Method, Stress, Safety Factor.

1. Introduction

The vehicle suspension system is a crucial component that plays a vital role in mitigating sudden and fluctuating loads, thereby ensuring the safety and longevity of various vehicle components. Fatigue failure, often initiated by the initial crack in these components, is a major concern. Therefore, suspension design is a meticulous process aimed at achieving optimal performance under maximum load conditions[1)]. The suspension generally relies on an ideal spring, which effectively serves its purpose as a damper[2)]. These dampers, commonly referred to as shock absorber, have the important task of dissipating energy generated by vertical movements resulting from uneven roads or wind[3)]. Additionally, they reduce spring oscillations and prevent excessive suspension motion [4)]. The oil valve within the suspension system is responsible for absorbing excess energy from the spring. It is crucial to acknowledge that the primary function of the spring is to store energy rather than dissipate or absorb it [5)]. When designing shock absorber, one key consideration is their ability to absorb energy effectively [6)]. Shock absorber also find application in safeguarding critical structures against shock and resonance effects in structural engineering[7)].

In various scientific and engineering domains, computational numerical simulations offer valuable solutions. For example, Finite Volume Method (FVM) was used to compute radiative information, the Lattice Boltzmann Method (LBM) was applied to solve the Energy equation, and Genetic Algorithms (GA) facilitated optimization [8,9)]. Moreover, the Adomian Decomposition Method (ADM) was used to address nonlinear governing differential equations for rectangular fins, accounting for temperature-dependent thermal conductivity and internal heat generation[9)]. Finite-Difference Method (FDM) was considered in order to obtain the required temperature field[10)]. Additionally, Finite Element Method (FEM) optimization was conducted for coil springs in automobile suspensions, comprising different material types[11),12)].

Numerous studies have investigated shock absorber behavior using FEM. For example, Duym conducted finite element analysis (FEA) of shock absorber models to establish relationships for manufacturing design acceptability based on static loading[13)]. Banginwar and Wang compared static structural analysis and modal analysis, varying spring component materials between

spring steel and phosphor bronze while evaluating the strengths of those materials[14,15].

In the studies mentioned above, boundary conditions were determined using static loading in FEA, showing its ability to clarify shock absorber behavior under stationary conditions. However, the use of cyclic loading for analysis offers increased precision and suitability as it reveals transient conditions during the process. In this current study, FEM was considered due to its capacity to address challenges related to discrete element, particularly complex structural models[12,16]. Additionally, the application of FEM proves highly effective for structural analysis, resulting in time and cost savings in laboratory experiments[17,18]. FEM analysis can optimize several component dimensions and material determinations for shock absorber modeling[19].

The prediction of stress concentration during cyclic loading of shock absorber holds significant importance in identifying critical points and areas exposed to cyclic loading during pre-load and load time intervals. This identification supports the early detection of potential defects in critical components. Therefore, this paper aims to predict stress levels and safety factor in shock absorber subjected to cyclic loading using FEM to observe transient conditions. Shock absorber model is initially constructed, and boundary conditions are defined with cyclic loading forces. Subsequently, mesh sizes are assessed and validated through grid independence and convergence testing. FEM facilitates the prediction of stress levels, deformations, and safety factor (SF).

2. Method

The study process for simulating shock absorber was shown in Figure 1 and it began with the design phase in CATIA software, where a model was derived from a commercial shock absorber for electric motorcycles. Before computation, the design was converted to STEP format and then exported to ANSYS software.

FEA consisted of three stages, namely pre-processing, analysis, and post-processing with result evaluation. The structural model went through modeling, and boundary conditions were also applied[20]. The mesh size was validated through mesh grid independence and convergence tests to determine the appropriate mesh size for model optimization and efficiency.

The simulation process was configured as transient static structural with a 20-second cycle. The results showed the response of the structure under cyclic loading, including stress, deformation, and safety factor. The simulation data, along with FEA results, were shown in tables, graphs, and plots. Stress distribution was visualized as a contour figure in the ANSYS software[21].

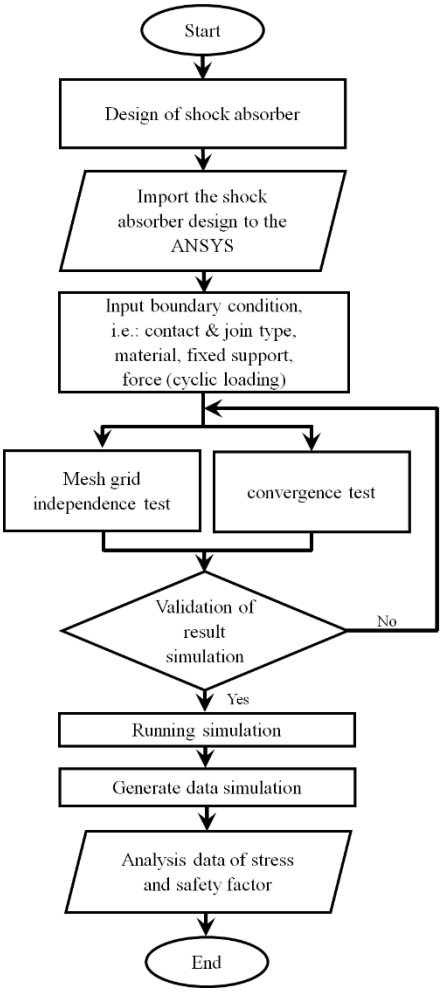

Fig. 1: Scheme of Simulation Process

2.1 Design and Material Assignment

Shock absorber modeled with licensed CATIA software is shown in **Fig. 2**.

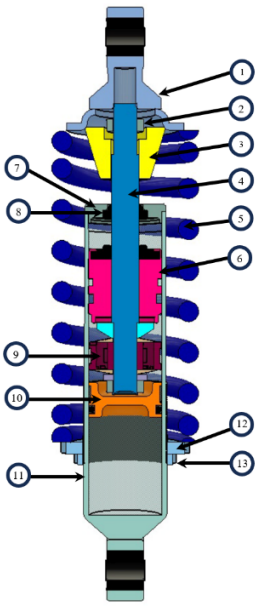

No	Part name	Material
1	Base Mount	Stainless steel, 17-4PH, cast, H1100
2	Lock Nut	Cast iron, BS grade Si 10 2
3	Adjuster Rod	Plastic, PA66 (40-45% mineral filled)
4	Piston Rod	Stainless Steel
5	Spring	Low alloy steel, 300M (low carbon)
6	Bumper	Aluminum Alloy
7	Dustcap	Stainless Steel
8	Seal valve	Rubber, nitrile (NBR)
9	Sandwich shim rubber	Rubber, PVC-elastomer (Shore A35)
10	Midvalve	Aluminum Alloy
11	Hydraulic Tube	Stainless steel, 201, 1/2 hard
12	Upper Adjuster	Aluminum Alloy
13	Lower Adjuster	Aluminum Alloy

Fig. 2: Model of Shock Absorber

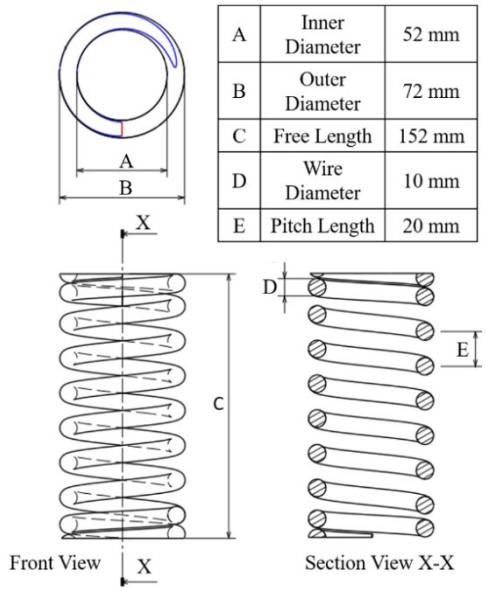

A	Inner Diameter	52 mm
B	Outer Diameter	72 mm
C	Free Length	152 mm
D	Wire Diameter	10 mm
E	Pitch Length	20 mm

Fig. 3: Spring Dimensions

Table 1. Material Properties of Spring

Parameters	Value
Material	Low carbon steel
Mass per wheel (***m***)	62.5 kg
Density	7.833e-06 kg/mm³
Young modulus	2.0555e+05 MPa
Tensile yield strength	1595 MPa
Stiffness coefficient (***k***)	1.73

The materials model was defined using a commercial motorcycle shock absorber method and experimental testing. Detailed material properties of shock absorber components were shown in **Fig. 2**, and spring dimensions could be seen in **Fig. 3**.

In the ANSYS software, contact geometry modeling assumed frictionless contact between components in the piston rod and the inner tube wall[22]. However, the contact in **Fig. 4** showed the stacking of components in the inner tube. From the visualization, it was apparent that the contact model was nearly invisible in the over-constrained part.

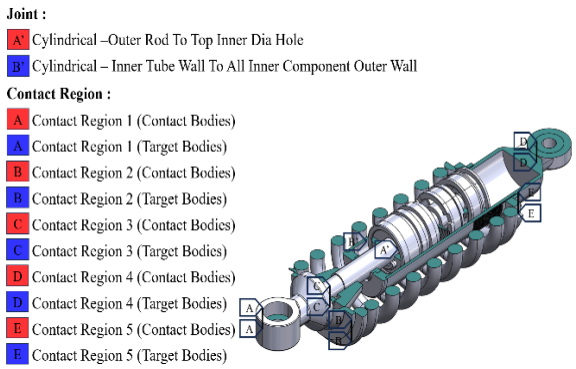

Fig. 4: Contact and Joint Constraints

2.2 FEM Analysis

This study method was used to address the complexity of shock absorber structures. At the core of FEM lay the relationship between the arranged stiffness matrix, which linked forces and displacements across the elastic region. Finite element discretization process computed strain and stress using the strain-displacement relationship and stress relationship[23].

Meshing was controlled using global and local mesh sizing. This study confined the meshing process to shock absorber model with swift transition and medium span angle center mesh settings. The bounding box calculation was based on geometric dimensions, with lengths represented as follows, including X = 71.99 mm, Y = 72.00 mm, and Z = 290.00 mm. The total surface area was 275.75 mm², and the minimum edge length was 0.2 mm. Mesh inflation was configured with a smooth transition and a ratio of 0.272, with a maximum layer value set to 5 and a growth rate of 1.2.

2.3 Load conditions

Shock absorber went through cyclic loading, with a cycle consisting of 20 steps within a 20-second period. It was designed to withstand a load of 125 kg, and the detailed information on the fixture force and load cycle graph could be seen in **Fig. 5 and 6.**

A load of 1250 N was applied to the upper mounting of shock absorber, with the mounting button serving as the fixed support. Moreover, the limitation of this study was the use of a 20-step cyclic load. The initial step was defined as preload, followed by the maximum load, and then shock absorber went through a rebound motion, with the spring returning to its starting position due to the load pressure. This process was repeated for a duration of 20 seconds, as shown in **Fig. 6**.

Each cycle of cyclic loading subjected shock absorber to compression and rebound, resulting in stress and deformation of its components. The amplitude and frequency of cyclic loads, along with the material properties of shock absorber components and its design, played a role in determining the load stress experienced by shock absorber.

To compute the load stress, basic mechanical principles were applied, defining stress *(σ)* as the force *(F)* exerted on an object divided by its cross-sectional area *(A)*:

$$\sigma = F/A \quad (1)$$

The force (F) was calculated as:

$$F = k.x \quad (2)$$

where k represents the stiffness coefficient of shock absorber and x is the compression displacement of shock absorber.

Fig. 5: Remote Force and Fixture

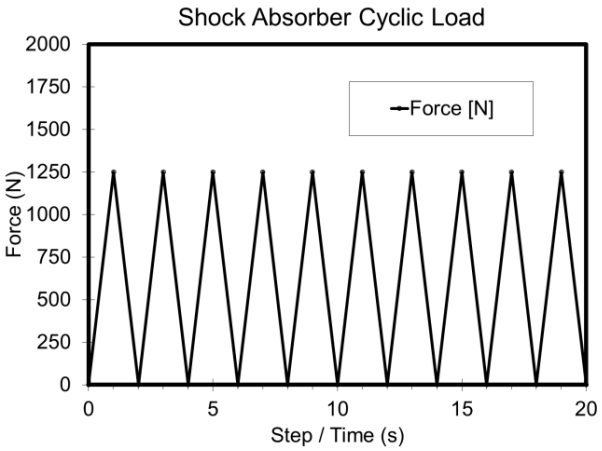

Fig. 6: Cyclic Load of Absorber

2.4 Meshing and Validation Method

Before selecting the mesh type and size for the simulation study, a mesh independence test was conducted. This test was defined by the grid of the mesh[24,25]. The results of the independence test for various mesh sizes are shown in Table 2, with Figure 7 showing the adjustments made to the grid mesh size, ranging from 3.25 to 2.00 mm with a 0.25 mm incremental value.

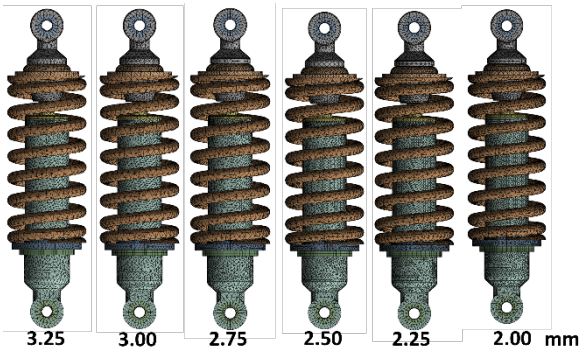

Fig. 7: Meshing Comparison

Table 2. Mesh grid independence test

Mesh Size	Nodes	Element	Max Def.	Max Stress
3.25	151964	76276	0.042	76.046
3.00	167801	85244	0.042	76.048
2.75	185732	94760	0.040	76.048
2.50	217803	112437	0.039	76.049
2.25	259853	133591	0.039	76.052
2.00	295265	152584	0.038	76.051
1.75	395175	209160	0.038	76.051
1.50	511086	276583	0.038	76.051

Changing the mesh size had adverse effects on the simulation runtime, making the grid independence test a reliable method for pre-processing simulation validation. As a general rule, when the results remain stable, the grid mesh parameter is considered sufficient. Deformation changes ranged from a 2.6% to a 4.7% decrease with mesh changes between 3.25, 3.00, 2.75, 2.50, and 2.25 mm. On the other hand, the variation in maximum stress levels gradually increased. With a mesh size of 2.00 mm, both deformation limits and maximum stress converged, leading to the selection of a 2.00 mm mesh size.

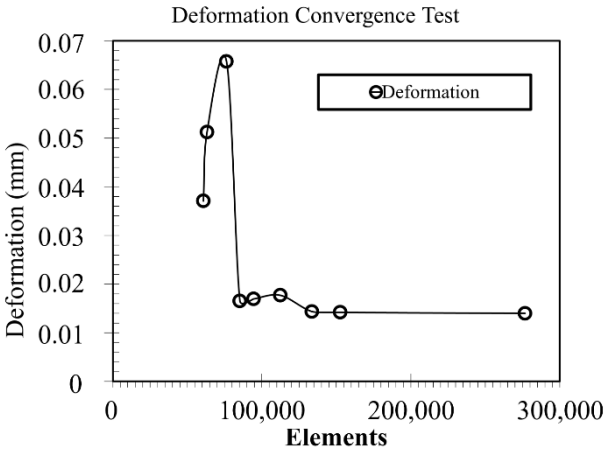

Fig. 8: Deformation Convergence Graph

In addition to the mesh independence test, a mesh convergence test was conducted to validate the accuracy of the simulation, as shown in **Fig. 8**. Various mesh sizes were selected to determine the solution for a specific position of shock absorber. The results were then compared to calculate the deviation between consecutive mesh sizes. Iterations were carried out with mesh sizes of 3.25, 3.00, 2.75, 2.50, 2.25, and 2.00 mm. Deformation was the selected parameter for observation. According to Kushwah[11], mesh convergence was achieved when the difference in deformation values is below 1%. The result showed that a 2.00 mm mesh size had a deviation of 0.49%, confirming its appropriateness.

3. Result and Discussion

The deformation process is based on the standard concept of viscoelastic phenomena in the material[26]. Shock absorber was deformed due to the compressive force on the upper mounting. **Fig. 9** and **Fig. 10** showed the deformation direction of vector and total deformation, respectively. The graphs showed the deformation value due to a load of 1250 N given in a cycle span of 20 steps. The maximum deformation on the upper spring was 0.039 mm. In comparison, the average value in the middle spring area was around 0.018 mm.

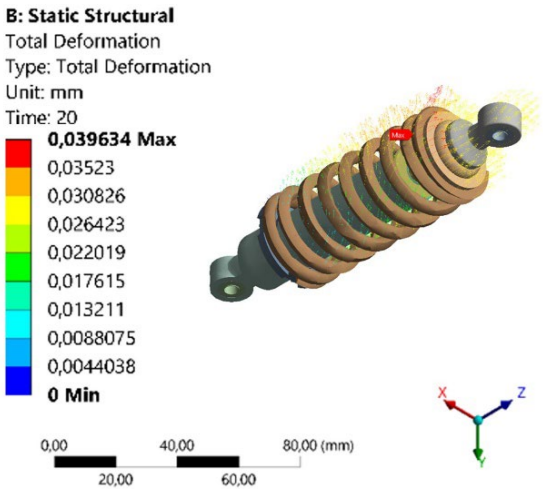

Fig. 9: Deformation Vector of Shock Absorber

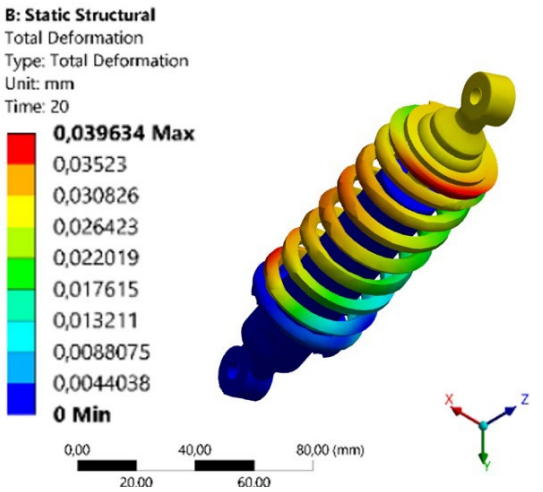

Fig. 10: Total Deformation of Shock Absorber

Figure 11 showed stress values within shock absorber, with the highest stress occurring at the upper adjuster, reaching approximately 77.382 MPa. Compressive forces tended to concentrate more than tensile forces, leading to areas of higher stress, especially where force was transferred or concentrated within the structure. This increased stress in specific areas contributed to the strength and stiffness degradation of the upper adjuster over the proposed cycle number[27]. Contact between the upper adjuster and the spring, along with frictional forces, significantly influenced stress distribution, particularly in critical areas where the spiral path was located. The tensile stress remained below the allowable yield stress for aluminum material (6061-T6), namely is 276 MPa[28], which was within safe limits. However, in long-term operation, areas with the highest von Mises stress may allow defects to develop over time. Gupta et al.[28] conducted stress analysis (von Mises) for various alloy materials and loading cases using ANSYS, concluding that aluminum alloys are lightweight but prone to deformation[29]. Therefore, components experiencing the highest von Mises stress should be reinforced in accordance with design safety standards, as a manufacturing consideration following ASME Standard[30].

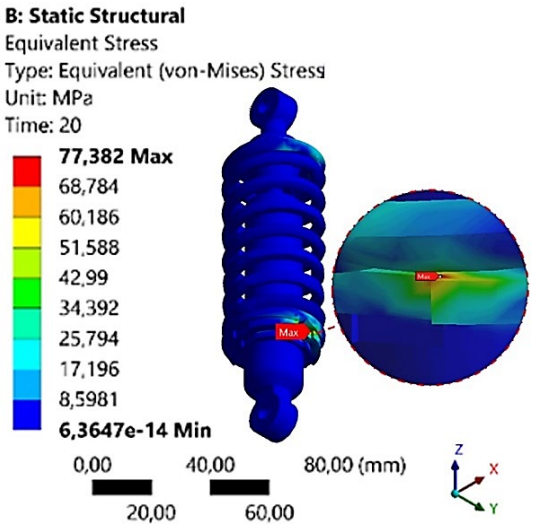

Fig. 11: Von-Misses Stress of Shock Absorber

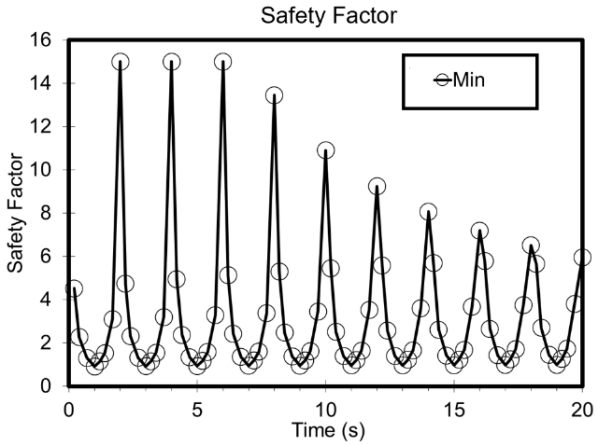

Fig. 12: Factor of Safety During Cyclic Load

Safety factor assisted in evaluating safety of a component or structure, even when using minimal dimensions[31]. It was the ratio between the yield strength of the material and the maximum von Mises stress. A design safety factor value of less than 1 indicated a design failure[32]. FEM simulation simplified the understanding of design failures by focusing on safety value of the design. Consequently, the results aided engineers in determining

the most appropriate safety factor. Figure 12 showed safety factor values over cyclic loading period of 20 seconds. The transient cyclic safety factor, represented by 80-time steps (equivalent to 20 seconds), exhibited a decreasing trend. The maximum safety factor, which initially peaked when shock absorber reached its zenith and returned to its pre-loading condition, began to decline after the sixth second. After 6 seconds of cycling, safety factor decreased by 89.66%, 72.66%, 61.58%, 53.76%, 47.93%, 43.39%, and 39.66%, respectively.

Fig. 13 showed a contour illustrating the prediction of safety factor distribution during transient cyclic loading with six located probes. The safest area was one with minimum stress, while the base mount was considered non-critical. It was the component in contact with upper positions, and the maximum achievable safety factor was 15. Although high safety factor values were present, local and secondary bending stress may still have existed, but these were permissible due to the application of a higher safety factor[33]. The minimum safety factor values could be seen in **Fig. 14**, with the average minimum safety factor being approximately 5.94, indicating that the design remained safe, as safety factor > 1.

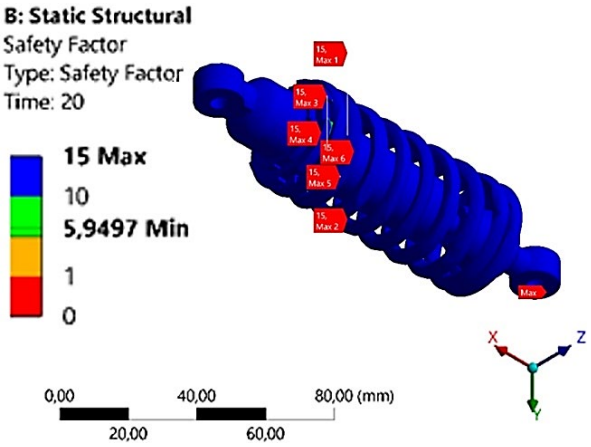

Fig. 13: Max safety factor of Shock Absorber

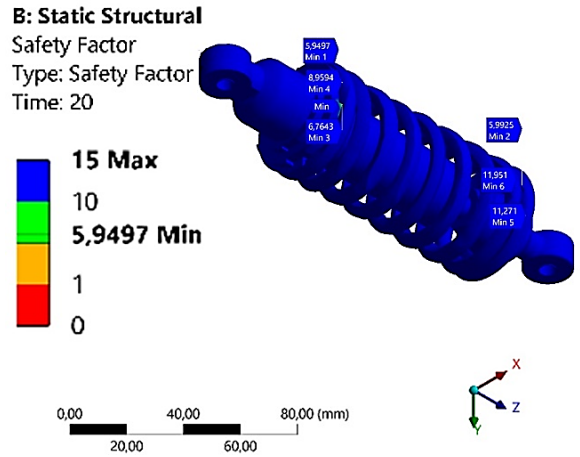

Fig. 14: Min safety factor of Shock Absorber

4. Conclusion

In conclusion, this study used numerical simulation to predict the strength of shock absorber and applied various material specifications to its sub-components. FEM simulation yielded results for von Mises stress, total deformation, and safety factor, which assisted in identifying critical areas within the components. The analysis comprised subjecting shock absorber to cyclic loads, which caused transient stress changes as it went through compressive stress and returned to its initial position every two seconds. This cycle continued until it reached 20 seconds, with two-second increments, resulting in stress values of 8.59, 17.174, 25.75, 34.23, 42.24, 49.84, 57.08, 64.02, 70.73, and 77.38 MPa, respectively. While the upper adjuster still had safety factor above the limit, it was identified as a potential early failure point compared to other components. This study successfully achieved its goals by predicting critical stress, deformation, and safety factor through simulation. The results described the importance of considering factor such as material treatment, manufacturing processes, and component lifespan in future analyses. Additionally, the possibility of coupling transient cyclic analysis with dynamic random vibration was explored to predict fatigue life in upcoming projects.

Acknowledgments

The authors are grateful to the Research Organization for Energy and Manufacture, National Research and Innovation Agency (BRIN) for supporting this investigation. All authors contributed equally to this work, actively participated in discussions about the results and their implications, and commented on the manuscript at all stages.

References

1) V. Trivedi, A. Saxena, M. Javed, P. Kumar, and V. Singh, "Design of six-seater electrical vehicle (golf cart)," *EVERGREEN Joint Journal of Novel Carbon Resource Sciences & Green Asia Strategy*, **10(2)** 953–961 (2023). doi.org:10.5109/6792890
2) P. Zheng, R. Wang, and J. Gao, "A comprehensive review on regenerative shock absorber systems," *Journal of Vibration Engineering and Technologies*, **8** (*1*) 225–246 (2020). doi:10.1007/s42417-019-00101-8.
3) J.C. Dixon, F.I.E. Mech, and F.R.S. Ae, "The Shock Absorber Handbook Second Edition," 2007.
4) C.H. Chin, S. Abdullah, S.S.K. Singh, A.K. Ariffin, and D. Schramm, "Durability assessment of suspension coil spring considering the multifractality of road excitations," *Measurement (Lond)*, **158** (2020). doi:10.1016/j.measurement.2020.107697.
5) A. Biradar, A. Patil, and K.K. Dhande, "Shock absorber design and analysis for off road race car," in:

Mater Today Proc, Elsevier Ltd, 2020: pp. 4997–5003. doi:10.1016/j.matpr.2020.12.941.

6) K. Venkata Siva Prasad, V. Nagasai, J. Sai Sri Laxman, K. v. Ahalya Kumar, and P.S. Rama Sreekanth, "Stainless steel wave spring as vibration absorber for motorcycle: design simulation and analysis," *Mater Today Proc*, 1056–1062 (2022). doi:10.1016/j.matpr.2021.09.289.
7) C.H. Chin, S. Abdullah, S.S.K. Singh, A.K. Ariffin, and D. Schramm, "On the need to evaluate the probabilistic of fatigue life assessment of random strain loading considering load sequence effects," *Eng Fail Anal*, **145** (2023). doi:10.1016/j.engfailanal.2022.107013.
8) R. Das, S.C. Mishra, M. Ajith, and R. Uppaluri, "An inverse analysis of a transient 2-d conduction-radiation problem using the lattice boltzmann method and the finite volume method coupled with the genetic algorithm," *J Quant Spectrosc Radiat Transf*, **109** (*11*) 2060–2077 (2008). doi:10.1016/j.jqsrt.2008.01.011.
9) R.K. Singla, and R. Das, "Application of adomian decomposition method and inverse solution for a fin with variable thermal conductivity and heat generation," *Int J Heat Mass Transf*, **66** 496–506 (2013). doi:10.1016/j.ijheatmasstransfer.2013.07.053.
10) R. Das, "Three-parameter estimation study in a radial fin geometry using FDM-based simplex method," in: Heat Transfer Engineering, 2014: pp. 1309–1319. doi:10.1080/01457632.2013.876866.
11) S. Kushwah, S. Parekh, and M. Mangrola, "Optimization of coil spring by finite element analysis method of automobile suspension system using different materials," in: Mater Today Proc, Elsevier Ltd, 2020: pp. 827–831. doi:10.1016/j.matpr.2020.11.415.
12) A. Jha, M. Soni, and M. Suhaib, "Non-invasive invitro modelling and finite elemental analysis of a uniquely designed prosthetic hand," *Evergreen*, **9**(*3*) 729–736 (2022). doi:10.5109/4843106.
13) S. Duym, R. Stiens, and K. Reybrouck, "Evaluation of shock absorber models," *Vehicle System Dynamics*, **27** (*2*) 109–127 (1997). doi:10.1080/00423119708969325.
14) A.P. Banginwar, N.D. Bhusale, and K. v Totawar, "Design and analysis of shock absorber using FEA tool," 2014. www.ijerd.com.
15) Y. Wang, K. Xu, and Q. Zhang, "Modal analysis and analysis of motor support based on workbench test bench design of motor dynamic shock absorber," in: J Phys Conf Ser, IOP Publishing Ltd, 2021. doi:10.1088/1742-6596/1986/1/012096.
16) E.D.P. Endra, A. Aziz, Dewi Rianti Mandasari, Lia Amelia, Agus Krisnowo, and Cuk Supriyadi Ali Nandar, "Analysis of bldc electric motor shaft treatment model using numerical method," *Majalah Ilmiah Pengkajian Industri*, **16** (*1*) (2022). doi:10.29122/mipi.v16i1.5263.
17) W. Libyawati, G. Kiswanto, A.S. Saragih, and T.J. Ko, "The influence of flexure variation to vibration-assisted micro-milling device by using finite element analysis," *Evergreen*, **9**(*2*) 577–583 (2022). doi:10.5109/4794205.
18) S.K. Lambha, V. Kumar, and R. Verma, "Impact of liner elasticity on couple stress lubricated partial bearing," *Evergreen*, **9** (*1*) 56–71 (2022). doi:10.5109/4774217.
19) S.L.S. Chauhan, and S.C. Bhaduri, "Structural analysis of a four-bar linkage mechanism of prosthetic knee joint using finite element method," *Evergreen*, **7**(*2*) 209–215 (2020). doi:10.5109/4055220.
20) C. Sai Kiran, "Design and analysis of shock absorber using ansys workbench," *CVR Journal of Science & Technology*, **17** (*1*) 144–149 (2019). doi:10.32377/cvrjst1725.
21) K. Balasubramanian, N. Rajeswari, and K. Vaidheeswaran, "Analysis of mechanical properties of natural fibre composites by experimental with FEA," in: Mater Today Proc, Elsevier Ltd, 2019: pp. 1149–1153. doi:10.1016/j.matpr.2020.01.098.
22) K.S. Phad, and A. Hamilton, "Experimental investigation of friction coefficient and wear of sheet metals used for automobile chassis," *EVERGREENJoint Journal of Novel Carbon Resource Sciences & Green Asia Strategy*, **9**(*4*) 1067–1075 (2022). doi.org:10.5109/6622880
23) G.D.C. Dhondt, "The finite element method for three-dimensional thermomechanical applications," Wiley, 2004.
24) W. Alt, "Mesh-Independence of the Lagrange-Newton Method for Nonlinear Optimal Control Problems and their Discretizations," 2001.
25) M.H. Pranta, M.S. Rabbi, S.C. Banik, M.G. Hafez, and Y.M. Chu, "A computational study on structural and thermal behavior of modified disk brake rotors," *Alexandria Engineering Journal*, **61** (*3*) 1882–1890 (2022). doi:10.1016/j.aej.2021.07.013.
26) K. Chen, H.W.B. Teo, W. Rao, G. Kang, K. Zhou, J. Zeng, and H. Du, "Experimental and modeling investigation on the viscoelastic-viscoplastic deformation of polyamide 12 printed by multi jet fusion," *Int J Plast*, **143** 103029 (2021). doi:10.1016/j.ijplas.2021.103029.
27) X. Cheng, T. Wang, J. Zhang, Z. Liu, and W. Cheng, "Finite element analysis of cyclic lateral responses for large diameter monopiles in clays under different loading patterns," *Comput Geotech*, **134** (2021). doi:10.1016/j.compgeo.2021.104104.
28) M.R. Gupta, and M.G.V.R.S. Rao, "Analysis of mountain bike frame by f.e.m," *IOSR Journal of Mechanical and Civil Engineering (IOSR-JMCE) e-ISSN*, **13** (*2*) 60–71 (2016). doi:10.9790/1684-1302026071.
29) A. Khechai, A. Tati, M.O. Belarbi, and A. Guettala, "Finite element analysis of stress concentrations in

isotropic and composite plates with elliptical holes," *Lecture Notes in Mechanical Engineering*, **789** 427–436 (2015). doi:10.1007/978-3-319-17527-0_43.

30) J. Yin, and X. Du, "A safety factor method for reliability-based component design," *Journal of Mechanical Design*, **143** (*9*) (2021). doi:10.1115/1.4049881.
31) L.A.N. Wibawa, "Effect of Fillet Radius of UAV Main Landing Gear on Static Stress and Fatigue Life using Finite Element Method," in: J Phys Conf Ser, IOP Publishing Ltd, 2021. doi:10.1088/1742-6596/1811/1/012082.
32) P. Castaldo, D. Gino, G. Bertagnoli, and G. Mancini, "Resistance model uncertainty in non-linear finite element analyses of cyclically loaded reinforced concrete systems," *Eng Struct*, **211** (2020). doi:10.1016/j.engstruct.2020.110496.
33) A. A. Faro, K. K. Salam, and E. E. Alagbe, "Design and analysis of a vertical pressure vessel with effect of rotational velocity on the stresses and deformation by using ansys," *International Journal of Analytical, Experimental and Finite Element Analysis (IJAEFEA)*, **6** (*3*) (2019). doi:10.26706/ijaefea.2.6.20190702.